Journal of Mechatronics, Electrical Power, and Vehicular Technology 17 (2026) 54-67

Journal of Mechatronics, Electrical Power, and Vehicular Technology

e-ISSN: 2088-6985
p-ISSN: 2087-3379

mev.brin.go.id

Stability challenge: Voltage profile enhancement and loss reduction using optimally placed single and dual SVCs

Latifa Smail [a, *], Hafidha Reriballah [b], Tadjeddine Ali Abderrazak [a], Guentri Hocine [a], Hari Maghfiroh [c], Medjdoubi Khadidja [a]

[a] *LSETER Laboratory, Technology Institute, Nour Bachir University Center El-Bayadh, 32000, Algeria*

[b] *Department of Electrical Engineering and automation, Faculty of Engineering, University Relizane Algeria*

[c] *Department of Electrical Engineering, Universitas Sebelas Maret Surakarta, 57126, Indonesia*

Abstract

High penetration of intermittent renewable energy sources (RES) fundamentally alters the voltage stability profile of electrical networks, creating significant challenges for regulation and efficiency. This paper investigates the optimal deployment of static var compensators (SVCs) to mitigate these instabilities in a 37-bus test system. The impact of integrating 15 MW of renewable generation is analyzed, comparing a PV-only scenario to a PV-wind hybrid system. A key contribution of this study is the comparative analysis between a centralized compensation strategy (using a single high-capacity SVC) and a distributed strategy (using dual SVCs with an equivalent total rating). Simulation results demonstrate that the distributed dual-SVC configuration is significantly more effective than the single-unit approach. This configuration ensures superior voltage stability, maintaining the minimum bus voltage above the critical threshold (≥ 0.9504 p.u.), and achieves a substantial 19.4 % reduction in active power losses. These findings confirm that distributing reactive power support provides a more robust solution for enhancing grid reliability and energy efficiency in hybrid renewable systems.

Keywords: static var compensator (SVC); power loss reduction; voltage stability; optimal FACTS placement; renewable energy integration; distributed compensation.

I. Introduction

In the current context of global energy development, electricity is a vital necessity, driving a rapid and continuous growth in demand. The widening gap between electricity supply and demand complicates the maintenance of voltage levels within required standards, leading to voltage instability and a degradation in the quality of energy transfer [1][2]. Also, dispatchers face a problem of voltage stability and frequency fluctuations, particularly during periods of high load. Nonlinear electrical load models under critical transient conditions play an essential role in the modelling and operating control equations of an electrical system. Maintaining a stable voltage within electrical networks is a significant challenge to ensure the reliability, quality and continuity of the power

* Corresponding Author. l.smail@cu-elbayadh.dz (L. Smail)

https://doi.org/10.55981/j.mev.2026.1317

Received 6 November 2025; 1st revision 28 January 2026; 2nd revision 9 February 2026; accepted 23 February 2026; available online 25 June 2026

How to Cite: L. Smail *et al.*, "Stability challenge: Voltage profile enhancement and loss reduction using optimally placed single and dual SVCs," *Journal of Mechatronics, Electrical Power, and Vehicular Technology*, vol. 17, no. 1, pp. 54-67, July, 2026.

supply [3]. It is therefore essential to maintain acceptable voltage levels on all buses, even after a disturbance, from an initial operating state. This ability defines what is called static voltage stability [4][5].

Faced with these challenges, the integration of renewable energy sources (RES, such as solar photovoltaic and wind) emerges as a promising solution due to their multiple environmental, and economic advantages [6][7][8]. However, the integration of these intermittent energy sources into existing electricity networks presents significant technical obstacles. In particular, reactive power support becomes critical, especially in the event of failure or sudden variation in production [9], this variability leads to fluctuations in power generation, which may result in supply instability and increase the risk of blackouts or service interruptions [10][11][12].

To overcome these limitations, the use of external devices such as flexible alternating current transmission systems (FACTS) is essential and effective in preventing voltage instability and collapse, thanks to their rapid action and high control flexibility at critical buses [13]. These devices are divided into four main categories according to their mode of connection to the network: series controllers such as the thyristor-commutated series capacitor (TSSC) and the thyristor-controlled series capacitor (TCSC) [14][15], shunt controllers including the static synchronous compensator (STATCOM), and the static reactive power compensator/static var compensator (SVC), which play a key role in regulating the voltage at critical buses and controlling the reactive power flow. Shunt capacitors are widely used for reactive power compensation [16][17].

They also play a crucial role in reducing power losses and enhancing the voltage profile in interconnected networks. In this category, the SVC remains one of the most widely used devices due to its relatively low cost and proven effectiveness in voltage regulation [18]. It is complicated and unnecessary to install shunt controllers on all buses for financial reasons, so it is crucial to identify strategic locations for their implementation [19][20][21].

Numerous studies in the literature have focused on the optimal placement of FACTS devices [17][18][19] using various algorithms and methods. Carlak and Kayar [20] used neural network based algorithms combined with meta-heuristic optimization (GA, particle swarm optimization (PSO)) for Volt/VAR regulation with SVC/STATCOM placement, while Astapov *et al.* [21] provided a comprehensive review of technical solutions addressing voltage and operational challenges in distribution grids with high intermittent RES, synthesizing control strategies and optimization approaches.

Similarly, Dandotia *et al.* [22] applied a genetic algorithm (GA) to determine the optimal position and sizing of an SVC for voltage profile improvement in renewable integrated systems. The strategic positioning of these devices has been shown to regulate power flows and maintain bus voltages within acceptable limits, thereby facilitating the integration of renewable energy sources, as demonstrated by Magadum *et al.* [23]; these results were also confirmed by other studies [24][25]. Furthermore, previous research confirms that integrating FACTS devices into power grids is an effective strategy for reducing total energy losses and mitigating voltage instability caused by factors like nonlinear loads and high renewable energy penetration, thereby improving overall power quality and system stability [26][27][28].

However, a critical review of the literature reveals a significant research gap. Most existing studies primarily concentrate on either determining the optimal location of a single FACTS device or generically analyzing their impact on system parameters. This approach overlooks a fundamental strategic question in grid planning: is it more effective to use a single, centralized high-capacity compensator or to distribute the same total compensation capacity across multiple, smaller units? Moreover, few studies have conducted a direct, systematic comparison of these two strategies, especially within the specific and increasingly relevant context of hybrid renewable energy systems (e.g., combined PV-wind) [29][30].

This paper directly addresses this gap by proposing a novel comparative framework. The core contribution of this work is a head-to-head evaluation of two SVC deployment strategies on a 37-bus test network: a single high-capacity SVC versus a distributed dual-SVC configuration with identical total reactive power rating. This analysis is conducted under two distinct renewable integration scenarios: a PV-only system and a hybrid PV-wind system. The primary objective is to determine whether a distributed compensation strategy offers superior performance in terms of voltage profile enhancement and active power loss reduction, thereby providing crucial insights for planning more resilient and efficient grids with high renewable penetration.

The remainder of this paper is structured as follows. Section 2 details the methodology, including the static modeling of the SVC, the power flow analysis, and the optimal location index. Section 3 presents and discusses the simulation results. The conclusions are summarized in section 4.

II. Materials and Methods

A. Static reactive power compensator

The SVC is a shunt-type FACTS device commonly used in transmission networks for voltage regulation and system stability improvement [29]. It consists of a capacitor bank and a thyristor-controlled reactor, connected in shunt. Its ability to rapidly inject or absorb reactive, capacitive, or inductive current allows dynamically adjusting the voltage at the bus to which it is connected. The SVC is typically modelled as a variable susceptance, depending on the firing angle of the thyristors. In this study, the single-line diagram of an SVC is shown in Figure 1, while the model of an SVC is shown in Figure 2.

Suppose an SVC is connected to bus k, the reactive power and current injected into bus k are calculated using equation (1) and equation (2) [30].

$$I_{svc} = jB_{svc}.V_k \quad (1)$$

$$Q_{svc} = Q_k = -V_k^2.jB_{svc} \quad (2)$$

where I_{SVC} and Q_{SVC} represent, respectively, the injected or absorbed reactive current and the reactive power supplied by the SVC, V_k is the voltage at bus k, and B_{SVC} is the susceptance. Equation (3) shows that the value of B_{SVC} can be regulated by adapting the triggering angle of the thyristors.

$$B_{svc} = \frac{X_l - \frac{X_c}{\pi}[2(\pi-\alpha)+\sin(2\alpha)]}{X_L X_c} \quad (3)$$

where X_l *and* X_c represent the reactance of the reactor and the capacitor, respectively, while α denotes the triggering angle of the thyristors.

The core of the control is a Proportional-Integral (PI) controller that works to eliminate the voltage error, as defined in equation (4).

$$\Delta B_{ref} = K_p\left(V_{ref} - V_i\right) + K_i \int_{\Re^+}\left(V_{ref} - V_i\right)d\tau \quad (4)$$

where K_p, K_i are proportional and integral gains, V_{ref} is set voltage (p.u.).

B. Operational limits

The SVC's susceptance is limited by its physical components, as expressed in equation (5):

$$B^{min} \leq B_{SVC} \leq B^{max} \quad (5)$$

The minimum susceptance limit can be given as in equation (6):

$$B^{min} = \begin{cases} -1.0\ p.u.\ if\ \ |Bc| < 10^{-5} \\ B_L/B_c \quad otherwise \end{cases} \quad (6)$$

where B_L is the inductive susceptance and B_c is the capacitive susceptance of the SVC.

C. Power flow analysis

The optimal power flow (OPF) aims to determine the best operating profile of the power grid by minimizing losses while satisfying the constraints of equality (power balance) and inequality (technical

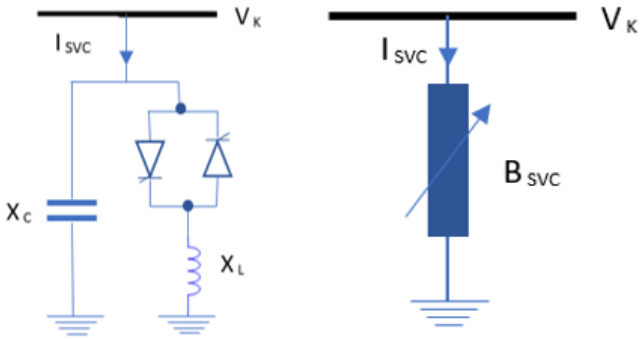

Figure 1. Single-line diagram of a classic SVC.

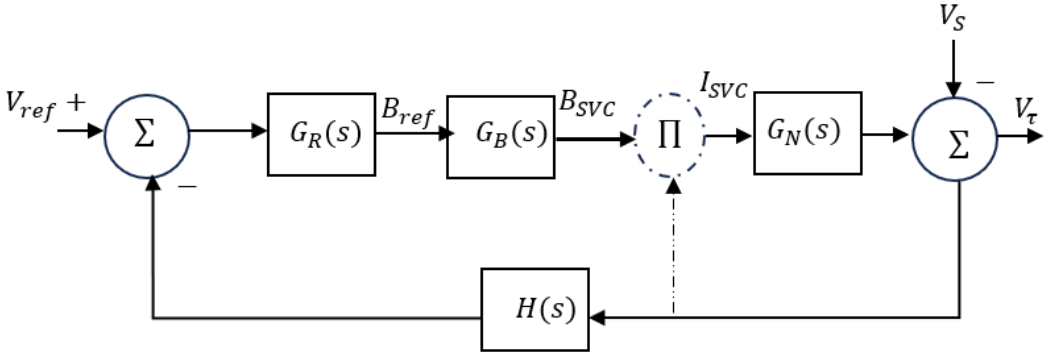

Figure 2. Equivalent model of an SVC.

limits of the system). The Newton-Raphson (NR) method was applied to model the power flow, both without and with the integration of renewable energy sources (RES), based on the SVC.

1) Power losses (PL)

$$P_G = P_{Load} + P_{loss} \quad (7)$$

$$Si = Pi + jQi \ , \ S_i^* = V_i^* * \left(\sum_{K=1}^{n} Y_{iK} V_K\right) \quad (8)$$

where P_G is the total generated active power, P_{Load} is the total load demand, P_{loss} is the total active power loss in the network, S_i is the complex power injected at bus i, P_i, Q_i are the active and reactive power injections at bus i respectively, V_i^* is the complex voltage at bus i, Y_{iK} represents the (i, k) -th element of the bus admittance matrix (Y_{bus}) of the power system , and n is the total number of buses in the network.

The active P_i and reactive power Q_i injected at a node are expressed by equation (9) and equation (10), respectively.

$$P_i = V_i(\sum_{K=1}^{n} Y_{iK} V_K) * cos(\theta_K + \delta_K - \delta i) \quad (9)$$

$$Q_i = -V_i(\sum_{K=1}^{n} Y_{iK} V_K) * sin(\theta_K + \delta_K - \delta i) \quad (10)$$

where V_i and V_k are the voltage magnitudes at buses i and k, respectively, θ_{ik} is phase angle of the admittance Y_{ik}, δ_i and δ_k are the voltage phase angles at buses i and k, respectively.

Minimizing active power losses in the network is a fundamental objective of OPF, which can be represented as shown in equation (11).

$$Min\ P_{Loss} = Min\{\sum_{i=1}^{NB}(P_{Gi}) - \sum_{i=1}^{NB}(P_{Di}) \quad (11)$$

where P_{Gi} is the active power generation at bus i, P_{Di} is the active power demand (load) at bus i, and NB is the number of buses.

$$Min\ P_{Loss} = Min\{\sum_{i=1}^{NB} G_{ij}\left[V_i^2 + V_j^2 - 2V_iV_j \cos(\delta_i - \delta_j)\right] \quad (12)$$

where G_{ij} is the conductance of the line between nodes i and j, V_i and V_j are the voltages at the transmitting and receiving ends, respectively, and δ_i, δ_j are the phase angles corresponding to these ends.

2) Equality constraints

The equality constraints of the OPF can be expressed as equation (13), equation (14), and equation (15):

$$P_{Gi} - P_{Di} - V_i \sum_{j=1}^{NB} V_j \left[G_{ij} \cos(\delta_{ij}) + B_{ij} \sin(\delta_{ij})\right] = 0 \quad \forall\ i \in NB \quad (13)$$

$$Q_{Gi} - Q_{Di} - V_i \sum_{j=1}^{NB} V_j \left[G_{ij} \sin(\delta_{ij}) - B_{ij}\cos(\delta_{ij})\right] = 0 \quad \forall\ i \in NB \quad (14)$$

$$Q_{Gi} - Q_{Di} \pm Q_{svc} - V_i \sum_{j=1}^{NB} V_j \left[G_{ij} \sin(\delta_{ij}) - B_{ij}\cos(\delta_{ij})\right] = 0 \quad \forall\ i \in NB \quad (15)$$

where, P_{Gi}, Q_{Gi} are active and reactive power generated at node i, Q_{Di}, P_{Di} are active and reactive power requested at node I, Q_{svc} is the reactive power injected into bus i by the svc, G_{ij}, B_{ij} are conductance and susceptance between nodes i and j.

3) Equality constraints

Inequality constraints represent the operational limits of the different components of the power grid. They can be formulated as follows:
Active and reactive generation limits represented as equation (16).

$$P_{Gi}^{min} \le P_{Gi} \le P_{Gi}^{max}, Q_{Gi}^{min} \le Q_{Gi} \le Q_{Gi}^{max} \quad (16)$$

Node voltage limits represented as equation (17).

$$V_i^{min} \le V_i \le V_i^{max} \quad (17)$$

Critical and marginal voltage represented as equation (18).

$$V_{min} \ge 0.90V \text{ (without SVC)}, V_{min} \ge 0.95V \text{ (with SVC)} \quad (18)$$

Line capacity limits represented as equation (19).

$$S_{ij} \le S_{ij}^{max} \quad (19)$$

SVC reactive compensation limits represented as equation (20).

$$Q_{svc}^{min} \le Q_{svc} \le Q_{svc}^{max} \quad (20)$$

Optimal location index: Identification of optimal location of SVC devices. The ideal location is determined by taking into account two opposing goals: improving the minimum voltage Vmin and reducing active losses P losses.

Equation (21) and equation (22) present the the objective functions for maximizing V_{min} and minimizing network power losses, respectively.

$$V_{norm,k} = \frac{V_{min,k} - V^{min}}{V^{max} - V^{min}} \quad (21)$$

$$P_{norm,k} = \frac{P^{max} - P_{loss,k}}{P^{max} - P^{min}} \quad (22)$$

where $V_{norm,k}$ is the normalized minimum voltage for candidate bus k (dimensionless), $V_{min,k}$ is the minimum bus voltage after compensation (p.u.), and V^{max}, V^{min} are the maximum and minimum voltages across all candidate buses (p.u.). $P_{norm,k}$ is the normalized power loss for candidate bus k

(dimensionless), $P_{loss,k}$ is the active power loss after compensation (MW), and P^{max}, P^{min} are the maximum and minimum losses across all candidate buses (MW).

The indicators are normalised, then they are associated using a weighted sum as given in equation (23).

$$\text{Performance Index (PI)} = \omega_v V_{norm,k} + \omega_p P_{norm,k} \quad (23)$$

with: $\omega_v + \omega_p = 1$ (ω_v =0.7 et $\omega_p = 0.3$).
where ω_v, ω_p are the relative weights given to voltage and losses, respectively.

A higher index value indicates better system performance, as it reflects both increased voltage profile stability and reduced active losses.

Optimal location can be expressed as equation (24).

$$k^* = \arg max_k \text{ Performance Index (PI)} \quad (24)$$

where k^* is the optimal bus index for SVC placement.

III. Results and Discussions

This section presents the simulation results of the 37-bus test system, including 9 generators, 26 load buses and 43 transmission lines. The integration of renewable energy sources was studied in two scenarios: without SVC and with SVC, by analyzing the voltage profile at the different buses as well as the losses in the network.

The total SVC capacity of 60 MVAR was selected based on a preliminary analysis of the network's reactive power requirements under worst-case (peak load, minimal renewable generation) and high renewable penetration scenarios. The sizing process involved:

- Running power flow for the base case (without RES or SVC) and identifying the buses with the most severe voltage violations.
- Calculating the approximate reactive power injection needed at the most critical bus to raise its voltage from the observed critical (~0.9 p.u.) to marginale level (>0.95 p.u.).
- Factoring in the additional reactive power support required to maintain stability after integrating 15 MW of intermittent renewable generation, which can create local voltage fluctuations.
- Considering typical SVC unit sizes and scaling to a value that represents a substantial yet realistic investment for the studied network. The 60 MVAR value represents approximately 8-10 % of the total system reactive load, aligning with practical rules-of-thumb for shunt compensation planning. The core comparative analysis remains valid as the same total compensation capacity (60 MVAR) is distributed between the single and dual SVC configurations.

A. Voltage control

1) Base case

Network without RES or SVC. Figure 3 illustrates the voltage profile obtained. According to the voltage profile results shown in Figure 3, the majority of bus

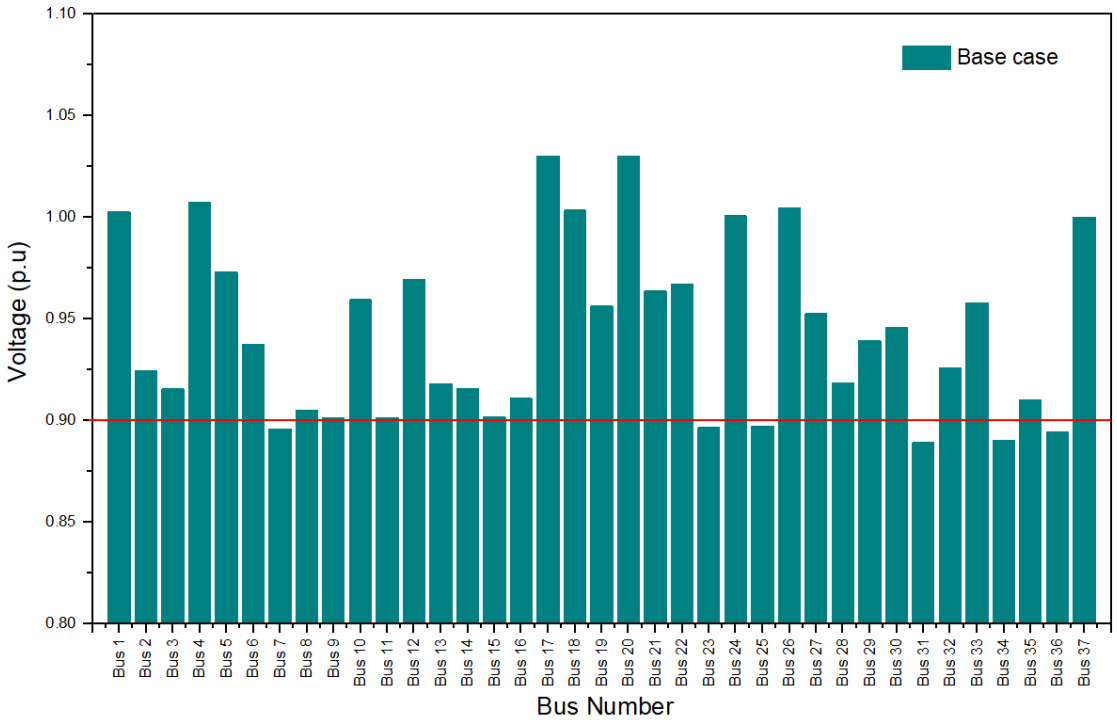

Figure 3. Voltage profile of the system without RES without SVC (base case).

voltages are between 1.03 p.u. and 0.90125 p.u.. However, six buses have critical values: bus 31 (0.88896 p.u.), bus 34 (0.89027 p.u.), bus 36 (0.89442 p.u.), bus 7 (0.89582 p.u.), bus 23 (0.89644 p.u.), and bus 25 (0.89715 p.u.).

2) Scenario 1: RES integration without SVC

The effect on voltage control was assessed by integrating 15 MW of photovoltaic (PV) generation at the critical buses of the 37-node network. Subsequently, a hybrid configuration combining PV and wind was studied, maintaining the exact total injected power as in the case of PV alone. The objective is to determine the optimal location of the units (PV then hybrid) to improve the network voltage profile.

The voltage at the different buses was expressed in relative units (p.u.) for the entire network. Figure 4 illustrates the voltage profile obtained for the integration of PV alone, without SVC, while Figure 5 presents the voltage profile corresponding to the hybrid PV–wind integration, also without SVC.

The analysis of the voltage profile curve shows that, compared to the base case, the integration of PV alone leads to a significant improvement in voltages on all buses, especially on the critical nodes initially undervoltage, with a minimum value of 0.91610 p.u observed at bus 31. Similarly, the hybrid PV–wind integration, with the same total injected power, further improves the voltage profile, reaching a minimum value of 0.92889 p.u. at bus 36.

3) Scenario 1: RES integration without SVC

The addition of SVC devices is studied in two configurations: a single high-capacity SVC (60 MVAR), optimally installed at the most critical node, and two SVCs sharing the same total power, distributed across two network buses. These configurations are evaluated in two distinct scenarios: the integration of a single photovoltaic (PV) source, and then that of a hybrid system (PV–wind).

The objective is to determine both the optimal location of the SVCs and the most efficient configuration (a single SVC or two SVCs), in terms of improving the voltage profile and reducing power losses in the network. Figure 6 and Figure 7 illustrate the voltage profile obtained for PV integration with 1 SVC and with 2 SVCs, respectively, while Figures 8 and 9 present the voltage profile corresponding to hybrid integration with 1 SVC and 2 SVCs, respectively.

According to the voltage profiles shown in Figure 6 and Figure 7, the placement of PV units at buses 31 and 34, whether in a configuration with one SVC or two SVCs, allows for an improvement in voltage across all buses. In this case, the minimum value recorded reaches 0.95 p.u. at bus 25, which ensures compliance with regulatory limits.

On the other hand, for other PV locations, the improvement remains partial: with a single SVC, the voltages at buses 31, 34 and 36 remain below the regulatory limit, while with two SVCs, it is buses 7, 31

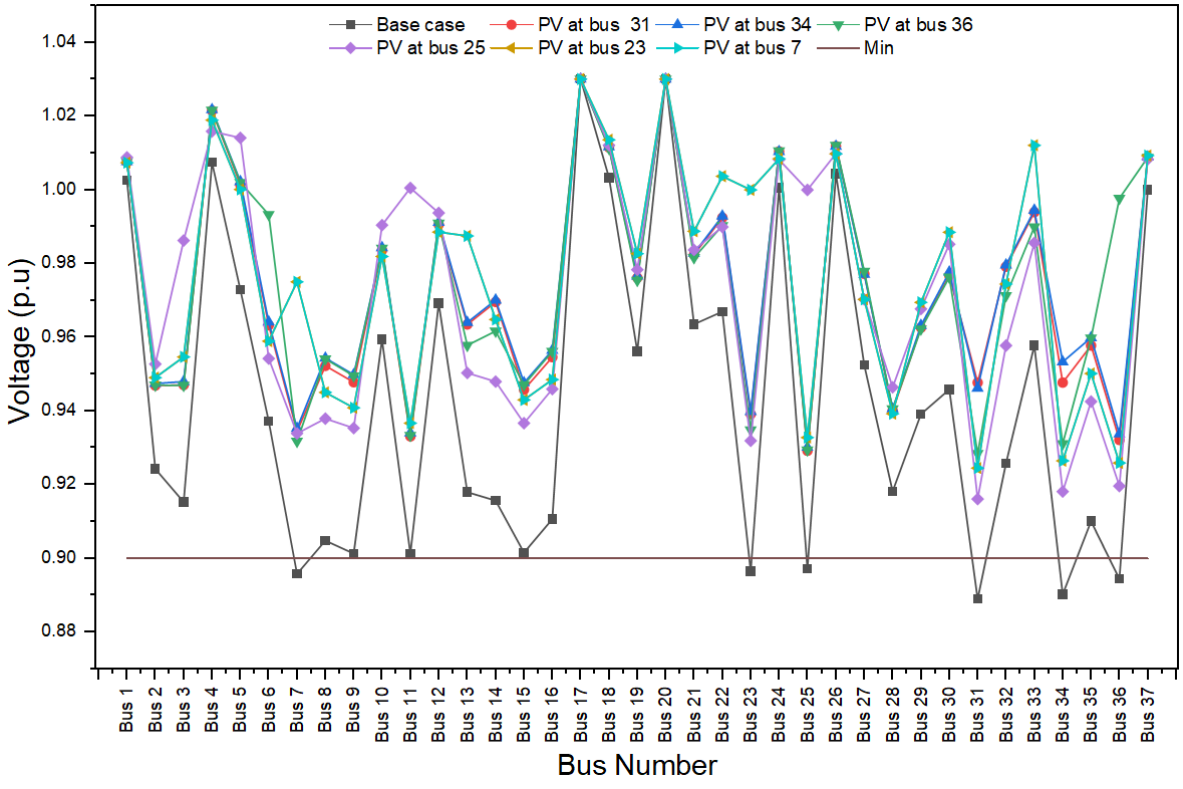

Figure 4. Voltage profile at the buses with renewable energy sources (PV) without SVC.

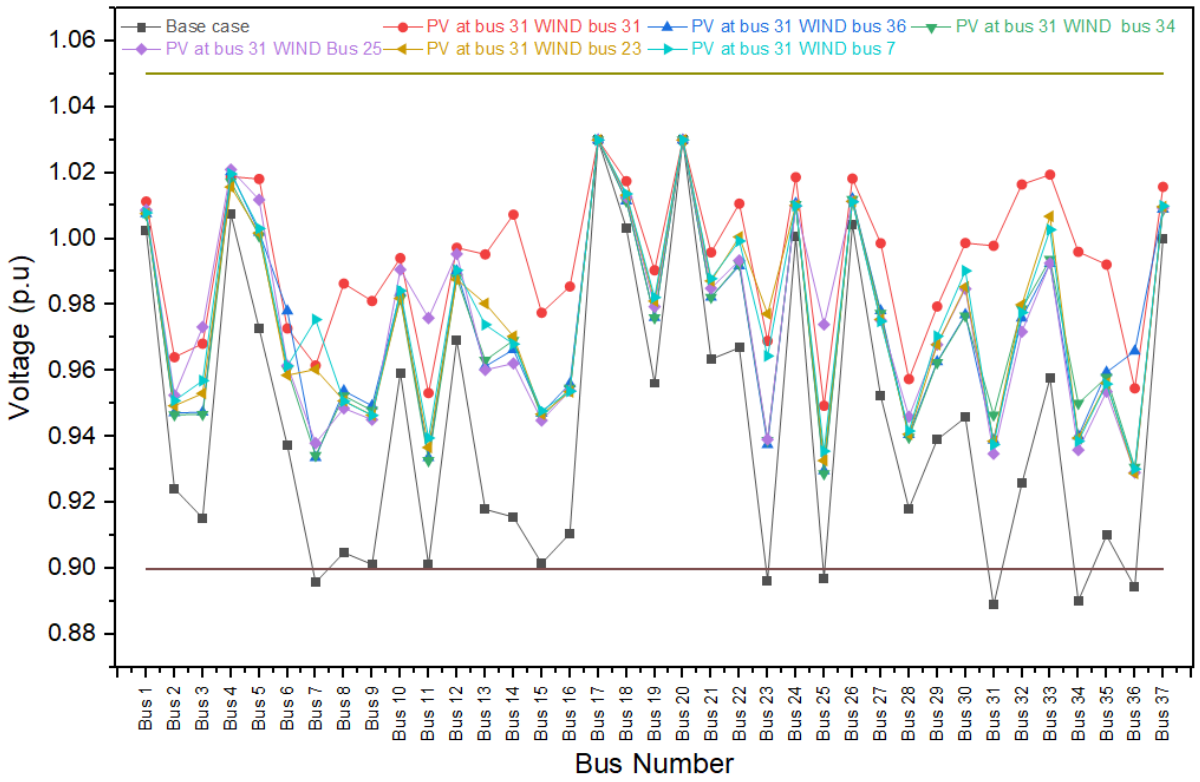

Figure 5. Voltage profile at the buses with renewable energy sources (hybrid) without SVC.

and 34 which remain below the regulatory limit. According to the voltage profile presented in Figure 8 and Figure 9, the integration of hybrid units, whether in a single SVC or dual SVC configuration, contributes to improving the voltage across all buses. With a single SVC, the lowest value noted is 0.94 p.u. at bus 36 for the scenarios where WIND is positioned at buses 23, 31 and 34 however, if the installation of an SVC at bus 36 or the integration of wind at buses 7, 25 and 36 (with an SVC at bus 25) contributes to improving the voltage across the entire network, with a minimum value of 0.95039 p.u. observed at bus 25. On the other hand,

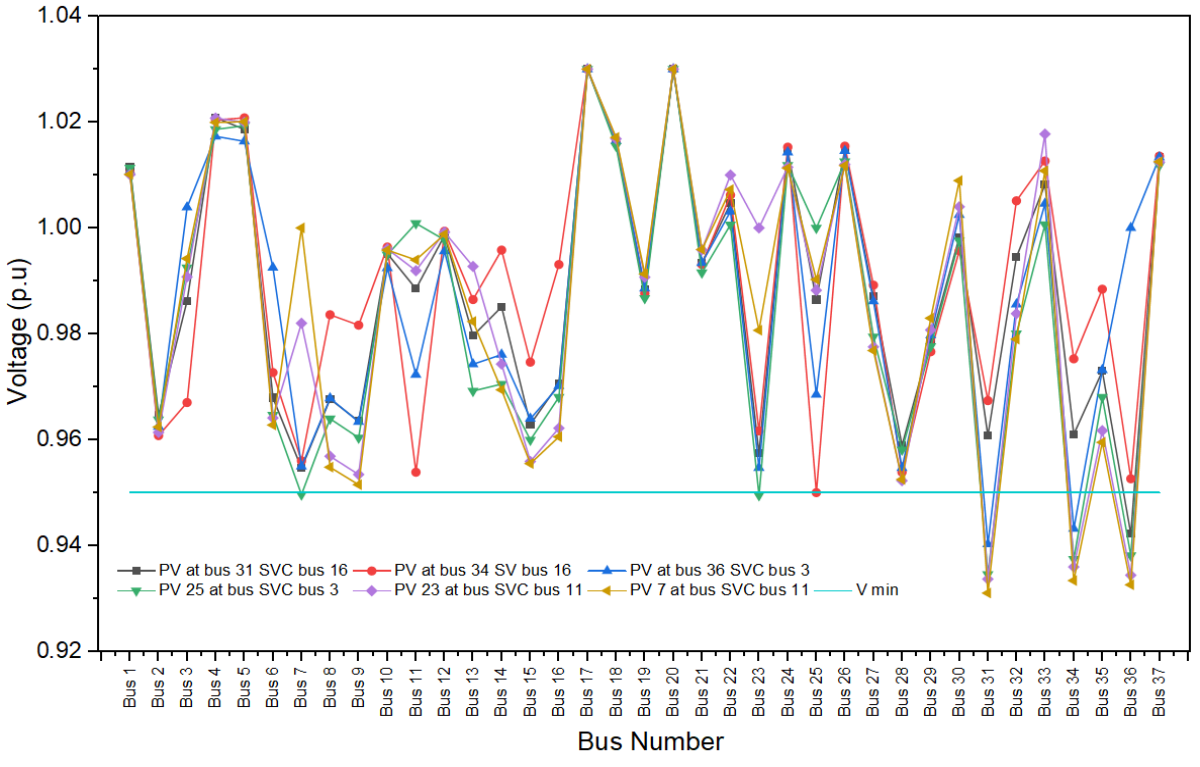

Figure 6. Voltage profile (p.u.) at the buses with PV with one SVC.

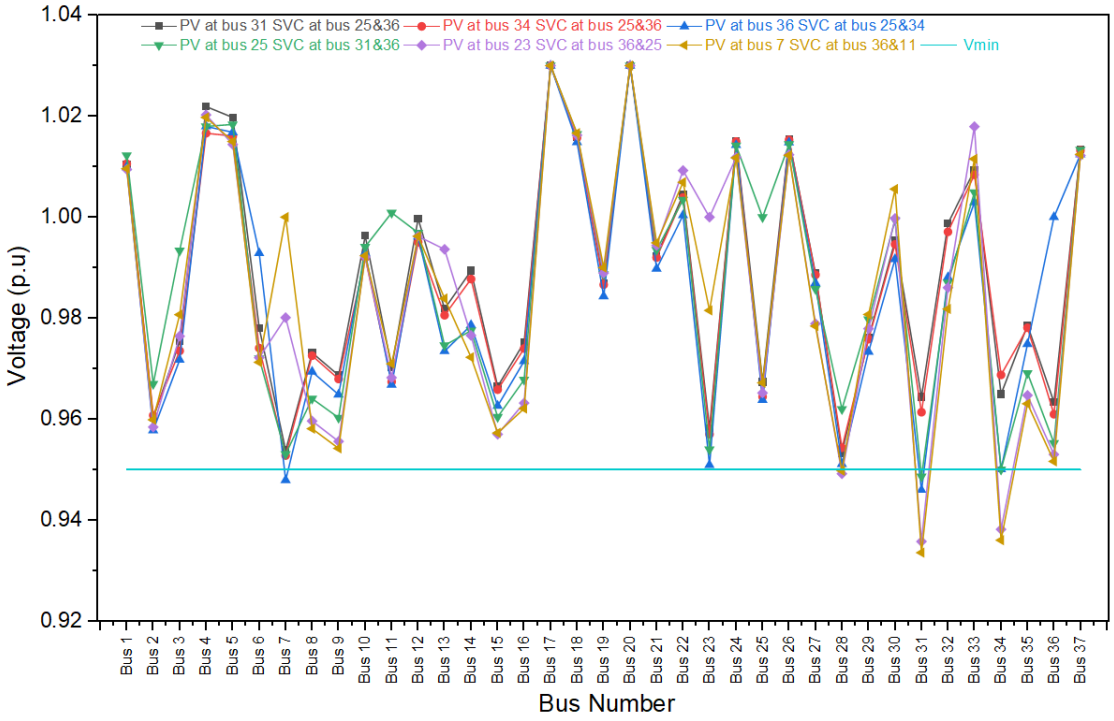

Figure 7. Voltage profile (p.u.) at the buses with PV with two SVCs.

with two SVCs, and for different locations of the PV and wind units, the voltages of all buses remain within the regulatory range of 0.95 p.u. to 1.05 p.u..

B. Power losses

The active power losses, for the cases with PV integration only and hybrid, before and after the installation of the SVC according to two possible arrangements (one or two SVCs), are presented in Figure 10 and Figure 11.

All critical network nodes integrating renewable sources (PV and hybrid) were analysed to determine the optimal location of the SVCs. The results show that after the installation of the SVC, active power losses are reduced. The minimum value recorded is 35.83 MW, obtained with two SVCs installed at buses 31 and 36, or with a PV connected to bus 25, a reduction of approximately 19.3 %.

A similar behaviour is observed for the hybrid case: a decrease in losses is observed when two SVCs are installed at buses 25 and 36, with a PV at bus 31 and a

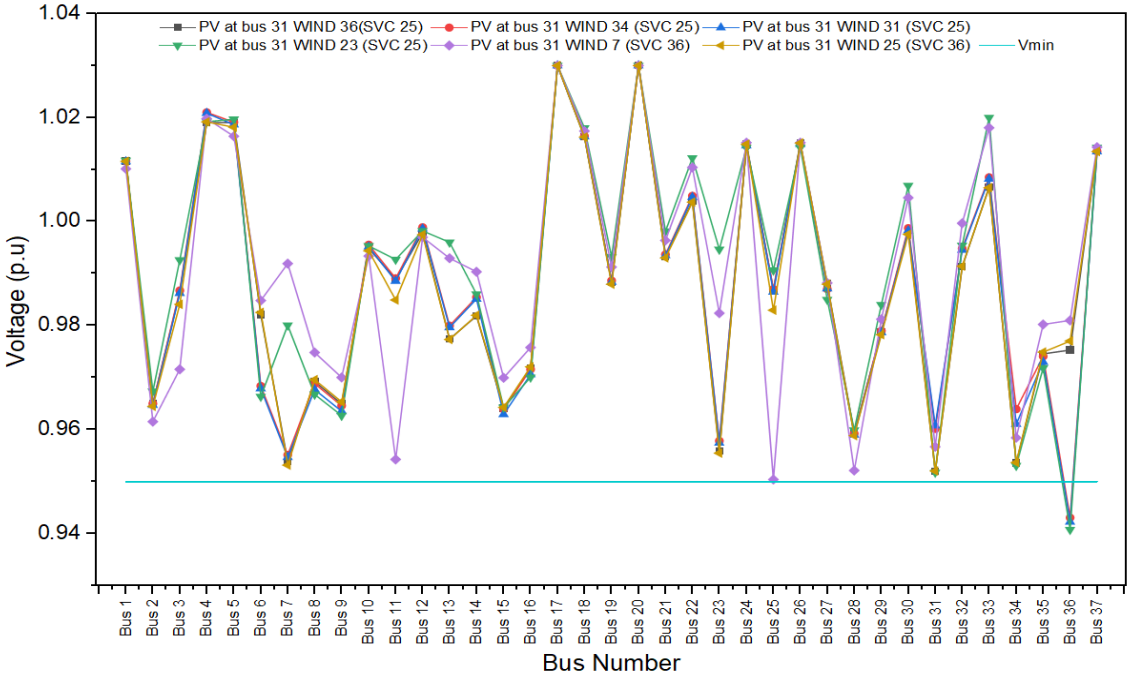

Figure 8. Voltage profile (p.u.) at the buses with (PV+wind + 1 SVC).

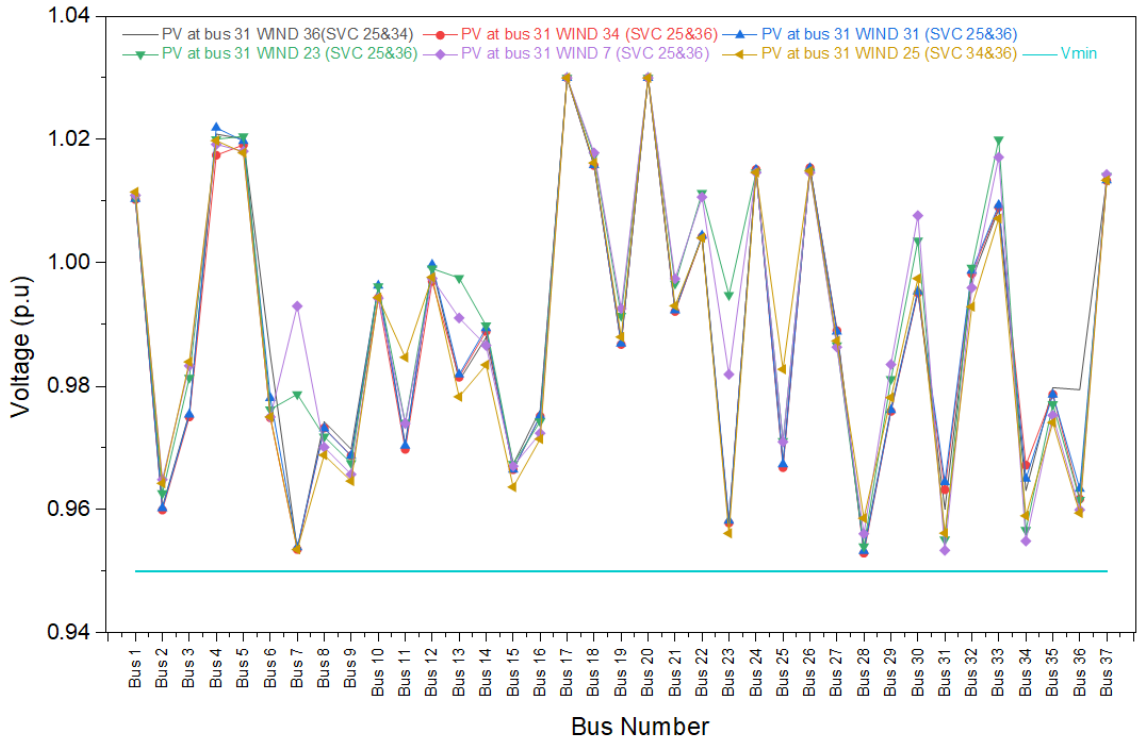

Figure 9. Voltage profile (p.u.) at the buses with (PV+wind + 2 SVCs).

wind turbine at bus 7; the losses decrease from 44.4 MW to 35.78 MW, which corresponds to a reduction of approximately 19.4 %.

C. Optimal placement analysis

The performance index (PI) developed in equations [21][22][23] provides a quantitative framework for comparing candidate locations, simultaneously rewarding voltage improvement and loss reduction. The weighting coefficients ($\omega_v = 0.7$, $\omega_p = 0.3$) reflect the regulatory priority of maintaining voltage within statutory limits (±5 %) while recognizing loss minimization as a secondary economic objective. Similar weighted-sum approaches have been successfully employed in recent FACTS allocation studies [31][32].

Table 1 presents the PI evaluation for the PV-only scenario without SVC. Among the six candidate buses exhibiting critical voltages in the base case, Bus 34 achieves the highest PI (0.973), driven by its superior post-integration voltage (0.93012 p.u.) and moderate losses (39.0 MW). Bus 31, despite having the lowest absolute losses (38.92 MW), receives a lower PI (0.951) due to its marginally lower voltage (0.92919 p.u.). This differentiation confirms the sensitivity of the weighted index to voltage violations. Buses 25, 23, and 7 score substantially lower (0.300–0.413), indicating that voltage improvement at these locations is achieved at the expense of significantly higher network losses or

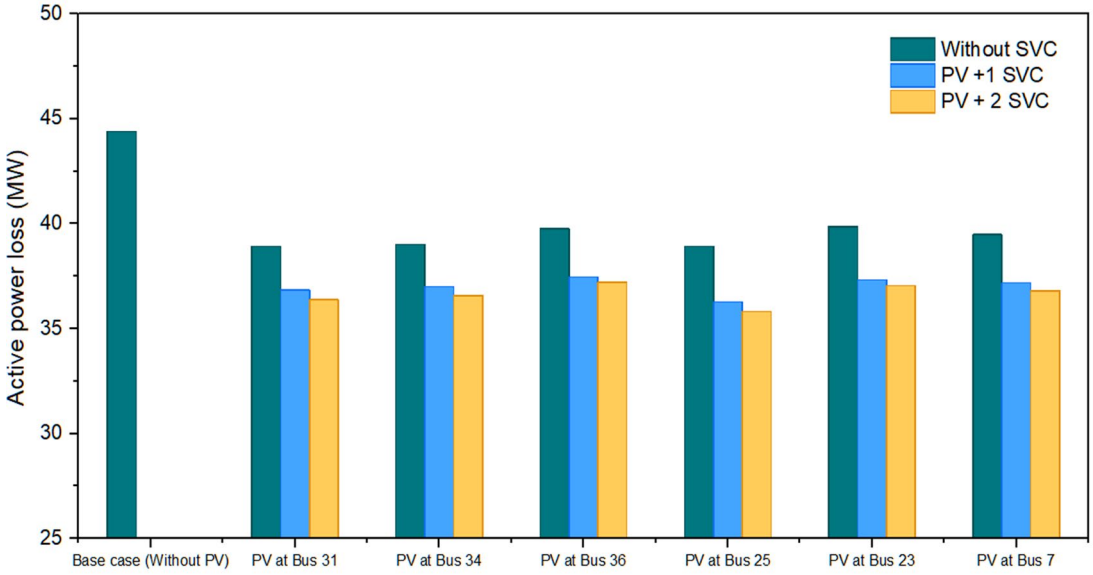

Figure 10. Bar chart showing the total real power loss of 37-bus power network (PV case).

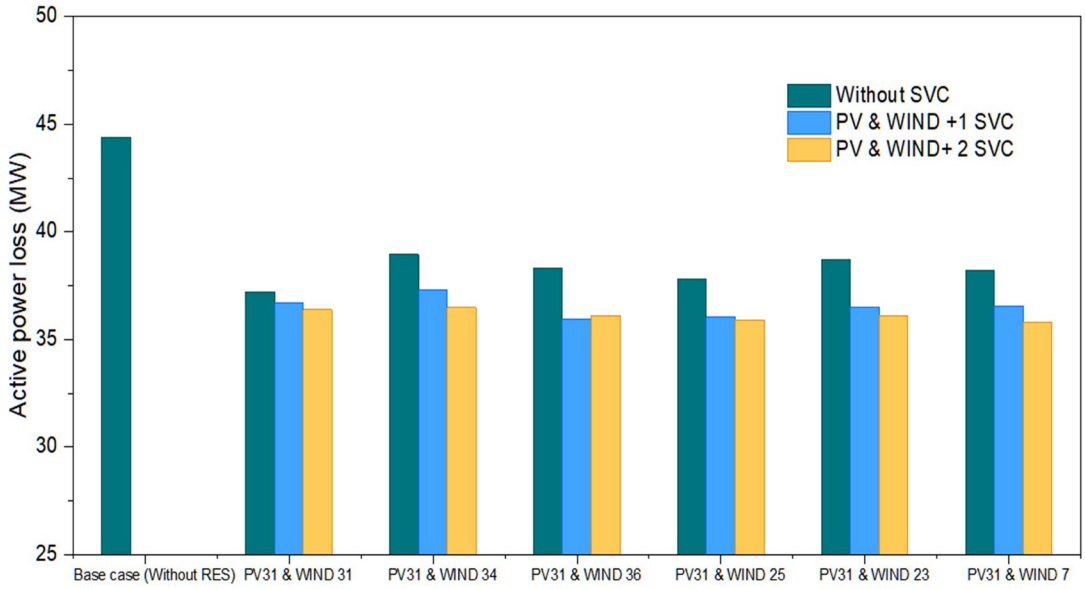

Figure 11. Voltage profile (p.u.) at the buses with PV with two SVCs.

insufficient voltage correction. The relatively low PI of Bus 36 (0.646) is noteworthy; although its voltage reaches 0.92848 p.u., losses increase to 39.76 MW, demonstrating that local voltage support can propagate adverse effects elsewhere in the network, a phenomenon documented in meshed systems with non-uniform loading [33][34].

Table 2 extends this analysis to the hybrid PV-wind configuration. The combination achieving both renewable sources at Bus 31 yields a dominant PI of 1.000, with minimum voltage reaching 0.94937 p.u, very near the 0.95 p.u. regulatory threshold, and losses reduced to 37.19 MW. All other hybrid placements exhibit substantially lower PI values (0.000–0.201). The zero score for placement (31 & 34) reflects the normalization process: this configuration produces the lowest Vmin (0.92878 p.u.) and highest losses (38.94 MW) among candidates, serving as the reference minimum. These results demonstrate that co-locating complementary renewable sources at a single strong bus maximizes voltage support, whereas geographically dispersing generation without coordinated reactive compensation can exacerbate voltage imbalances.

Table 3 evaluates SVC deployment in the PV-only system. The dual-SVC configuration at Buses 25 and 36 (with PV at Bus 31) achieves the maximum normalized

Table 1.
Evaluation of the PI to identify the optimal location without SVC (PV case).

Location	Bus 31	Bus 34	Bus 36	Bus 25	Bus 23	Bus 7
V min	0.92919	0.93012	0.92848	0.9161	0.92449	0.92179
Loss (MW)	38.92	39	39.76	38.92	39.86	39.48
Performance index (PI)	0.951	0.973	0.646	0.3	0.413	0.4

Table 2.
Evaluation of the PI to identify the optimal location without SVC (hybrid).

Location	31 & 36	31 & 34	31 & 25	31 & 23	31 & 7	31 & 31
V min	0.92969	0.92878	0.92917	0.92889	0.93021	0.94937
Loss (MW)	38.31	38.94	37.83	38.68	38.23	37.19
Performance index (PI)	0.139	0	0.201	0.045	0.161	1

Table 3.
The PI evaluation for optimal SVC location identification (PV and SVC).

Location	PV with SVC			
	At bus 31		At bus 34	
SVC number	1 SVC	2 SVCs	1 SVC	2 SVCs
V min	0.95	0.9533	0.95001	0.95284
Loss (MW)	36.84	36.38	37.01	36.58
Performance index (PI)	0.078	1	0.0021	0.731

Table 4.
The PI evaluation for optimal SVC location identification (hybrid system with 1-SVC).

Location	Hybrid (PV and wind)		
	31 & 36	**31 & 7**	**31 & 25**
SVC number	1 SVC	1 SVC	1 SVC
V min	0.95195	0.95039	0.95204
Loss (MW)	35.96	36.55	36.02
Performance index (PI)	0.53	0	0.524

Table 5.
The PI evaluation for optimal SVC location identification (hybrid system & 2-SVCs).

Location	Hybrid (PV, Wind)					
	31 & 36	**31 & 34**	**31 & 25**	**31 & 23**	**31 & 7**	**31 & 31**
SVC number	2 SVC	2 SVC	2 SVC	2 SVC	2 SVC	2 SVC
V min	0.95355	0.95294	0.95353	0.95402	0.95339	0.9533
Loss (MW)	36.09	36.47	35.89	36.12	35.78	36.38
Performance index (PI)	0.788	0.522	0.862	0.867	0.878	0.626

PI of 1.000, with Vmin = 0.9533 p.u. and losses = 36.38 MW. In contrast, the single 60 MVAR SVC at Bus 31 yields PI = 0.078, near the minimum of the normalized range, despite achieving the 0.95 p.u. threshold. This dramatic disparity reveals a fundamental limitation of the single-SVC strategy: while it corrects the local voltage at the installation bus, it fails to provide adequate support to electrically remote nodes, forcing those buses to operate near the regulatory limit. The dual-SVC configuration, by distributing compensation, raises the entire voltage profile and reduces circulating reactive currents, explaining both the improved Vmin and reduced losses. This finding directly supports the central hypothesis that distributed compensation outperforms centralized schemes.

Table 4 examines single-SVC deployment in the hybrid system. The configurations with PV at Bus 31 and Wind at Bus 36 (SVC at Bus 25) and PV at Bus 31 with Wind at Bus 25 (SVC at Bus 36) achieve comparable PI values (0.53 and 0.524 respectively). Both maintain minimum voltages above 0.951 p.u. and losses near 36.0 MW. Notably, the configuration with Wind at Bus 7 achieves the regulatory 0.95 p.u. threshold (0.95039 p.u.) but receives a normalized PI of zero, indicating it is the weakest performer among the evaluated candidates.

Table 5 presents the dual-SVC hybrid results; the first table in this study to demonstrate universal regulatory compliance. All six tested renewable placement combinations maintain Vmin ≥ 0.95294 p.u., comfortably above the 0.95 p.u. threshold. The PI values cluster between 0.522 and 0.878, with the optimal configuration being dual SVCs at Buses 25 and 36, PV at Bus 31, and Wind at Bus 7 (PI = 0.878, losses = 35.78 MW). This configuration achieves the lowest absolute losses among all hybrid scenarios and a 19.4 % reduction relative to the best-performing hybrid configuration without SVC (Table 2, 37.19 MW). Critically, the dual-SVC configuration at Buses 25 and 36 appears repeatedly as the optimal or near-optimal compensator placement across both PV-only and hybrid scenarios, suggesting this bus pair represents a structurally advantageous location for distributed compensation in the 37-bus test system.

D. Summary of optimal placement results

These results consistently demonstrate that distributed compensation through optimally placed dual SVCs provides superior voltage regulation and loss reduction compared to centralized single-SVC deployment, regardless of whether the renewable generation is PV-only or hybrid PV-wind, distinguishing between the PV-only and Hybrid scenarios:

1. PV-only scenario

- Without SVC: The optimal location for the PV generator is at Bus 34.
- With Single SVC: When PV is connected to Buses 31 and 34, the optimal location for a single SVC is at Bus 16.
- With Dual SVC: The optimal locations for two SVCs are Buses 25 and 36 (with PV at Bus 31).
- Overall Best Configuration: Considering both loss reduction and the overall PI, the superior configuration is Dual SVCs installed at Buses 25 and 36, with the PV generator connected to Bus 31.

2. Hybrid (PV-wind) scenario

- Without SVC: The optimal configuration corresponds to both the PV and Wind units connected to Bus 31.
- With Single SVC :
  If PV is at Bus 31 and Wind is at Bus 7 or 25, the optimal SVC location is Bus 36.
  If Wind is connected to Bus 36, the optimal SVC location shifts to Bus 25.
- With Dual SVC: All tested locations successfully maintained voltage within regulatory limits.

Overall Best Configuration: In terms of power loss reduction and overall score, the optimal solution is Dual SVCs installed at Buses 25 and 36, with the PV generator at Bus 31 and the Wind turbine at Bus 7.

IV. Conclusion

This paper addressed the critical challenges of voltage instability and power losses in distribution networks under high penetration of renewable energy. By strictly comparing a centralized single-SVC approach against a distributed dual-SVC configuration with identical total capacity, this study provides clear evidence for the superiority of distributed reactive power support. The simulation results on the 37-bus test system demonstrate that the optimal placement of dual SVCs, particularly within a hybrid PV-wind scenario, yields the most robust performance. This configuration successfully maintained all bus voltages above the critical threshold (≥ 0.9504 p.u.) and achieved a substantial 19.4 % reduction in active power losses. Crucially, the analysis revealed that while a single high-capacity SVC can improve local voltage profiles, it fails to adequately address voltage drops at electrically remote nodes. In contrast, the distributed dual-SVC strategy effectively mitigates these limitations, offering a more resilient solution for managing the intermittency of renewable generation. These findings advocate for the adoption of distributed FACTS strategies in modern grid planning. Future work will extend this research to include dynamic stability analysis under fault conditions and a detailed economic assessment of the proposed hybrid configurations.

Declarations

Author contribution

Latifa Smail, Hafidha Reriballah, Tadjeddine Ali Abderrazak, Guentri Hocine, Hari Maghfiroh, and Medjdoubi Khadidja contributed equally as the main contributors of this paper. All authors read and approved the final paper.

Funding statement

This research did not receive any specific grant from funding agencies in the public, commercial, or not-for-profit sectors.

Competing interest

The authors declare that they have no known competing financial interests or personal relationships that could have appeared to influence the work reported in this paper.

The use of AI or AI-assisted technologies

During the preparation of this work, the author(s) used Gemini in order to improve the language clarity, grammar, and academic tone of the manuscript. After using this tool/service, the author(s) reviewed and edited the content as needed and take(s) full responsibility for the content of the publication.

Additional information

References

[1] A. M. Saleh, I. Vokony, M. Waseem, M. A. Khan, A. Al-Areqi, "Power system stability with high integration of RESs and EVs: Benefits, challenges, tools, and solutions", *Energy Reports*, 13, 2637–2663, 2025.

[2] A. A. Tadjeddine, I. Arbaoui, R. I. Bendjillali, A. Chaker, "Enhancing power grid reliability with AGC and PSO: Insights from the Timimoun Photovoltaic Park", *EAI Endorsed Transactions on Energy Web*, Vol. 12, 2024.

[3] S. Sharma, S. Gupta, M. Zuhaib, V. Bhuria, H. Malik, A. Almutairi, A. Afthanorhan, M. A. Hossaini," A comprehensive review on STATCOM: Paradigm of modeling, control, stability, optimal location, integration, application, and installation", *IEEE Access*, Vol. 12, pp. 2701–2729, 2024.

[4] S. Mokred, Y. Wang, "Comparative analysis of voltage stability in radial power distribution networks under critical loading conditions and diverse load models", *Electricity*, 6(4), 64, 2025.

[5] T. A. Abderrazak, B. R. Ilyas, B. M. Sofiane, H. Hichem, A. Iliace, "Advanced dynamic stability system developed for nonlinear load", *International Journal of Power Electronics and Drive Systems/International Journal of Electrical and Computer Engineering*, 14(4), 2032, 2023.

[6] S. K. Suraparaju, M. Samykano, J. R. Vennapusa, R. K. Rajamony, D. Balasubramanian, Z. Said, A. K. Pandey, "Challenges and prospectives of energy storage

integration in renewable energy systems for net zero transition", *Journal of Energy Storage*, 125, 116923, 2025.

[7] A. Mohammed, E. K. Sakr, M. Abo-Adma, R. Elazab, "A comprehensive review of advancements and challenges in reactive power planning for microgrids", *Energy Informatics*, 7(1), 2024.

[8] M. R. D. Abdilla, N. A. Windarko, B. Sumantri, "Photovoltaic energy harvesting booster under partially shaded conditions using MPPT based sand cat swarm optimizer," *Journal of Mechatronics, Electrical Power, and Vehicular Technology*, *15*(1), 42-56, 2024.

[9] E. E. Che, K. R. Abeng, C. D. Iweh, G. J. Tsekouras, A. Fopah-Lele, "The impact of integrating variable renewable energy sources into grid-connected power systems: Challenges, mitigation strategies, and prospects," *Energies*, 18(3), 689, 2025.

[10] S. J. Yeboah, S. Nunoo, J. C. Attachie, W. D. Asihene, E. Y. Asuamah, "Impact and integration techniques of renewable energy sources on smart grid operations: A systematic review," *Scientific African*, 29, e02845, 2025.

[11] K. K. Lusimbakio, T. B. Lokanga, P. S. Nzakuna, V. Paciello, J. N. Nsekere, O. T. Tshipata, "Evaluation of the impact of photovoltaic solar power plant integration into the grid: A case study of the western transmission network in the Democratic Republic of Congo," *Energies*, 18(3), 639, 2025.

[12] M. Mudakir, A. Aripriharta, A. P. Wibawa, "Analysis of battery energy storage system [BESS] performance in reducing the impact of variable renewable energy generation intermittency on the electricity system," *Journal of Mechatronics, Electrical Power, and Vehicular Technology*, *15*(2), 158-176, 2024.

[13] R. Gadal, A. Oukennou, F. E. Mariami, A. Belfqih, N. Agouzoul, "Voltage stability assessment and control using indices and FACTS: A comparative review," *Journal of Electrical and Computer Engineering*, 1–18. 2023.

[14] B. H. Alajrash, M. Salem, M. Swadi, T. Senjyu, M. Kamarol, S. Motahhir, "A comprehensive review of FACTS devices in modern power systems: Addressing power quality, optimal placement, and stability with renewable energy penetration," *Energy Reports*, 11, 5350–5371. 2024.

[15] A. Carbonara, S. D. Sessa, A. L'Abbate, F. Sanniti, R. Chiumeo, "Comparison of advanced flexible alternating current transmission system (FACTS) devices with conventional technologies for power system stability enhancement: An updated review," *Electronics*, 13[21], 4262, 2024.

[16] E. F. Fuchs, M. A. Masoum, "The roles of filters in power systems and unified power quality conditioners," *In Elsevier eBooks*, pp. 915–1016, 2023.

[17] I. A. Khan, H. Mokhlis, N. N. Mansor, H. A. Illias, L. J. Awalin, L. Wang, "New trends and future directions in load frequency control and flexible power system: A comprehensive review," *Alexandria Engineering Journal*, 71, 263–308, 2023.

[18] V. Saxena, S. Manna, S. K. Rajput, P. Kumar, B. Sharma, M. H. Alsharif, M. Kim, "Navigating the complexities of distributed generation: Integration, challenges, and solutions," *Energy Reports*, 12, 3302–3322, 2024.

[19] I. Marouani, T. Guesmi, B. M. Alshammari, K. Alqunun, A. S. Alshammari, S. Albadran, H. H. Abdallah, S. Rahmani, "Optimized FACTS devices for power system enhancement: Applications and solving methods," *Sustainability*, 15(12), 9348, 2023.

[20] H. F. Carlak, E. Kayar, "Volt/VAR regulation of the West Mediterranean regional electrical grids using SVC/STATCOM devices with neural network algorithms," *Wind Energy*, 28(2), 2025.

[21] V. Astapov, N. Shabbir, A. Rosin, L. Kütt, V. Maask, & H. Tiismus, "Review of technical solutions addressing voltage and operational challenges in a distribution grid with high penetration of intermittent RES," *Energy Reports*, 14, 1738–1760, 2025.

[22] A. Dandotia, M. K. Gupta, M. K. Banerjee, S. K. Singh, B. Đurin, D. Dogančić, N. Kranjčić, "Optimal Placement and Size of SVC with Cost-Effective Function Using Genetic Algorithm for Voltage Profile Improvement in Renewable Integrated Power Systems," *Energies*, 16(6), 2637, 2023.

[23] R. B. Magadum, C. J. Sudhakar, A. V. Deshpande, S. N. Dodamani, "Optimal placement of multiple STATCOM and its impact on voltage stability," *in 2021 7th International Conference on Advanced Computing and Communication Systems (ICACCS),* Coimbatore, India, pp. 238–242, Mar. 2021.

[24] A. T. Alemu, G. M. Meseret, "Optimal location and sizing of static VAR compensator [SVC] to improve voltage profile in distribution network," *Engineering Reports*, 7(10), 2025.

[25] W. Chen, Y. Fan, J. Lin, X. Fang, X. Huang, Z. Li, J. Yuan, F. Xiao, D. Zhang, J. Jiang, G. Ma, "A review on the application of D-FACTS devices for power quality optimization in distribution networks," *Measurement and Control*, 2025.

[26] C. Valuva, S. Chinnamuthu, "A taxonomical review: recent advancements in FACTS controllers on power systems with modern optimization techniques," *Computers & Electrical Engineering*, 123, 110120, 2025.

[27] M. T. Hagh, M. a. J. Borhany, K. Taghizad-Tavana, M. Z. Oskouei, "A comprehensive review of flexible alternating current transmission system (FACTS): Topologies, applications, optimal placement, and innovative models," *Heliyon*, 11(1), e41001, 2024.

[28] H. Iqbal, A. Stevenson, A. I. Sarwat, "Impact analysis and optimal placement of distributed energy resources in diverse distribution systems for grid congestion mitigation and performance enhancement," *Electronics*, 14[10], 1998, 2025.

[29] T. Sarkar, S. Gupta, C. Paul, S. Dutta, P. K. Roy, A. Bhattacharya, G. G. Tejani, S. J. Mousavirad, "Optimal allocation of STATCOM for multi-objective ORPD problem on thermal wind solar hydro scheduling using driving training-based optimization," *Scientific Reports*, 15(1), 19594, 2025.

[30] T. F. Etanya, P. Tsafack, D. K. Ngwashi, "Grid-connected distributed renewable energy generation systems: Power

quality issues, and mitigation techniques – A review", *Energy Reports*, 13, 3181-3203, 2025.

[31] S. S. Reddy, "Optimal placement of FACTS controllers for congestion management in the deregulated power system," *International Journal of Electrical and Computer Engineering (IJECE)*, 8(3), 1336, 2018.

[32] A. Sahoo, P. K. Hota, P. R. Sahu, F. Alsaif, S. Alsulamy, T. S. Ustun, "Optimal congestion management with FACTS devices for optimal power dispatch in the deregulated electricity market," *Axioms*, 12[7], 614, 2023.

[33] M. H. Sulaiman, Z. Mustaffa, "Optimal placement and sizing of FACTS devices for optimal power flow using metaheuristic optimizers," *Results in Control and Optimization*, 8, 100145, 2022.

[34] Z. Cheng, L. Wang, C. Su, R. Zhang, X. Li, B. Zhang, "Data-driven coordinated voltage control strategy for distribution networks with high proportion of renewable energy based on voltage–power sensitivity," *Sustainability*, 17(11), 4955, 2025.